JACS
JOURNAL OF THE AMERICAN CHEMICAL SOCIETY
Article
pubs.acs.org/JACS

Cyclo-Pnicta-triazanes: Biradicaloids or Zwitterions?

Alexander Hinz,[†] Axel Schulz,*[,†,‡] Alexander Villinger,[†] and Jan-Martin Wolter[†]

[†]Institut für Chemie, Abteilung Anorganische Chemie, Universität Rostock, Albert-Einstein-Strasse 3a, 18059 Rostock, Germany

[‡]Leibniz-Institut für Katalyse e.V., Universität Rostock, Abteilung Materialdesign, Albert-Einstein-Strasse 29a, 18059 Rostock, Germany

Supporting Information

ABSTRACT: Bulky triazenides were utilized in the reaction with pnictogen(III) chlorides (ECl_3, E = P, As, Sb, and Bi) yielding triaza-pnicta-butene analogues of the type R−N═N−N(R)−ECl_2 (R = Ter = 2,6-bis(2,4,6-trimethylphenyl)phenyl). Subsequent reduction of these dichloro-species afforded unprecedented four-membered group 15 heterocycles [E(μ-NTer)$_2$N] bearing one dicoordinate pnictogen and nitrogen atom. These N_3E rings represent species at the borderline between singlet biradicaloids and zwitterions with diminished reactivity compared to known singlet biradicaloids. The N_3P compound could be identified, while N_3As and N_3Sb species as well as the precursor compounds were fully characterized.

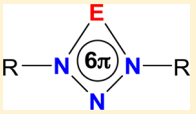

INTRODUCTION

Ever since the discovery of the first phosphorus(III)-nitrogen heterocycle, [ClP(μ-NR)]$_2$ (**A**, Scheme 1), by Michaelis and Schröter,[1] binary pnictogen-nitrogen heterocycles have been in the focus of main group chemistry.[2−4] Starting from [ClP(μ-NR)]$_2$, an eight π electronic system with all pnictogen being tricoordinate (Scheme 1), we recently isolated the six π electronic *cyclo*-dipnictadiazane-1,3-diyls [(μ-NTer)E]$_2$ (E = P, As; Ter = 2,6-bis(2,4,6-trimethylphenyl)-phenyl) by reduction with magnesium.[5,6] Thus, we raised the question if it is possible to replace one pnictogen E by nitrogen to form the hitherto unknown pnictatriazane-1,3-diyls [E(μ-NTer)$_2$N] (E = P, As, Sb, Bi). Of special interest seemed to be the study of the electronic structure with respect to the nature of the six π electronic system, whether a large biradical character (formula **B**)[2,6−30] and enlarged reactivity is observed or zwitterionic Lewis structures (e.g., formulas **C** and **D**) dominate accompanied by a lower reactivity. Due to the involvement of a triazenide backbone, the targeted species should be even more strained heterocycles and feature an unprecedented bonding situation. A related N_3P heterocycle was only recently investigated by Scheer et al., which was prepared by addition of alkyl azides onto the phosphinidene complex Cp*P[W(CO)$_5$]$_2$.[31] Because of the existence of two additional substituents compared to our envisaged target molecules [E(μ-NTer)$_2$N], the bonding situation is fundamentally different.

Scheme 1. Synthesis and Bonding of *Cyclo*-Dipnicta-diazane-1,3-diyls [(μ-NR)E]$_2$ (E = P, As; R = Ter = 2,6-bis(2,4,6-trimethylphenyl)phenyl)

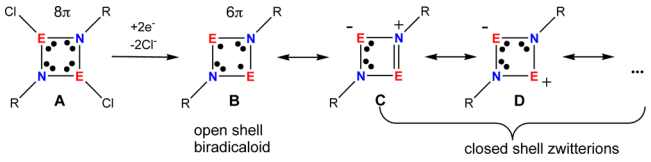

To generate the novel N_3E heterocycles according to Scheme 1 (with one E = N), the unknown dichloro precursors R−N═N−N(R)−ECl_2 had to be isolated first, as we did not see a chance to prepare the analogous dichloro compounds **A** (Scheme 1) with one N−Cl bond. Hence, triazenides have been considered as valuable ligands for at least two reasons: Due to their two organic substituents they possess tunable bulkiness, and electron delocalization can lead to redox noninnocence. Groundbreaking work in this field was carried out by Niemeyer et al.,[32−36] who investigated several ionic triazenides with various organic substituents, e.g., with alkaline or alkaline earth cations as counterions. Despite or maybe even due to their intriguing ligand properties, there are no investigations regarding the chemistry of triazenides with respect to the late main group elements, especially group 15.

RESULTS AND DISCUSSION

Adopting literature protocols for triazenide synthesis,[32−37] it was possible to generate the symmetric lithium triazenide, $Ter_2N_3Li(OEt_2)$ (**1**) by reaction of TerLi with $TerN_3$ in Et_2O. **1** is a versatile starting material (Scheme 2). The conversion with ECl_3 (E = P, As, Sb, Bi) leads to the formation of $Ter_2N_3ECl_2$ (**2E**). In case of **2P** (E = P, Scheme 2), this species is only stable at low temperatures ($\delta[^{31}P]$ = +178 ppm, cf. $TerPCl_2$ +161, $TerNHPCl_2$ +159 ppm)[38,39] since it rearranges above −40 °C, leading to the formation of **3P** ($\delta[^{31}P]$ = −46 ppm, Figure 1), which is elusive and tends to eliminate N_2 so that finally $TerPCl_2$ was obtained. Attempts to prepare **2P** via base-induced elimination of HCl from a mixture of triazene Ter_2N_3H (**5**) and PCl_3 were not successful. Furthermore, the conversion of **1** with PI_3 resulted in a decomposition product as well, and diiododiphoshadiazane [IP(μ-NTer)]$_2$ was obtained (cf. SI). However, in situ generated **2P** can be utilized for the reduction process to give **4P** ($\delta[^{31}P]$ = +342 ppm, Scheme 2).

Received: January 28, 2015
Published: March 6, 2015

DOI: 10.1021/jacs.5b00959
J. Am. Chem. Soc. 2015, 137, 3975−3980

Scheme 2. Synthesis of 2E (E = P, As, Sb, Bi), 3P, and 4E (E = P, As, Sb)

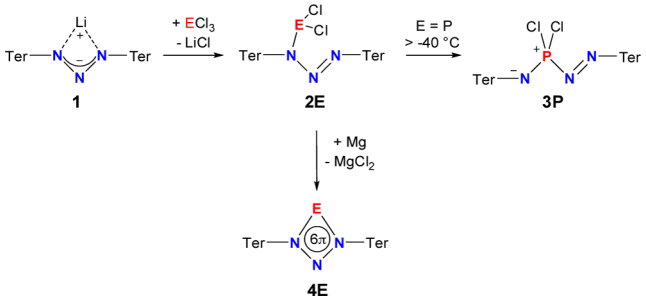

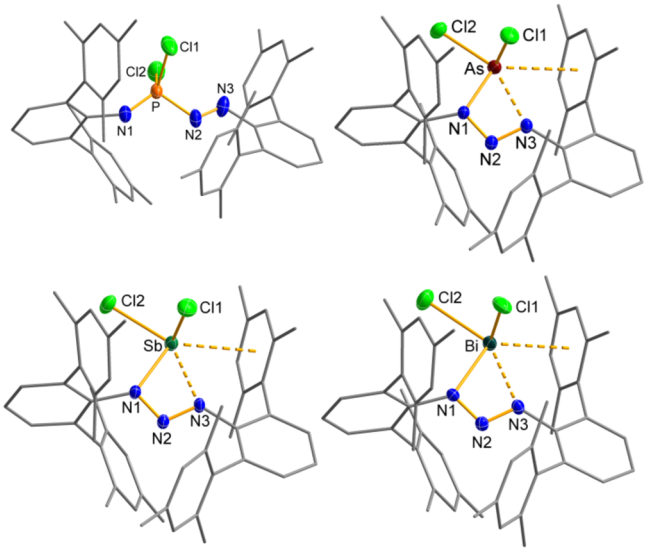

Figure 1. Molecular structures of **3P**, **2As**, **2Sb**, and **2Bi**. Selected bond lengths in Å: P–N1 1.498(4), P–N2 1.743(3), P–N3 2.513(2); As–N1 1.937(1), As–N2 2.643(1), As–N3 2.344(1); Sb–N1 2.153(2), Sb–N2 2.792(1), Sb–N3 2.408(2); Bi–N1 2.286(2), 2.873(1), 2.451(2). Thermal ellipsoids are drawn at 50% probability (173 K).

In all other cases **2E** (E = As, Sb, and Bi; Figure 1) was isolated from benzene and fully characterized.

In any case, **2E** can easily be reduced with magnesium or KC_8 to form **4E** (Scheme 2, Figure 2) in good yields except for deep red **4Bi** which stays elusive and decomposes within minutes. While yellow **4P** always cocrystallized with considerable amounts of the triazene Ter_2N_3H (**5**), pure **4As** (yellow crystals) and **4Sb** (red crystals) could be isolated. The UV–vis spectra of **2E** and **4E** show distinct absorptions in the near UV range that can be attributed to π–π^* transitions (vide infra). These bands are bathochromically shifted upon reduction. The HOMO → LUMO excitations cause the intense yellow color of **4As** and the red color of **4Sb** (λ_{max}(**4As**) = 332, 413; λ_{max}(**4Sb**) = 352, 506; cf. λ_{max}(**2As**) = 340, 379; λ_{max}(**2Sb**) = 341, 383 nm).

Vibrational spectra of **2** and **4** feature two different N–N stretching modes (Table 1), in accord with computational frequency analysis by means of DFT (M06-2X/aug-cc-pvdz level). Interestingly, for **2** the coupling between both N–N stretching modes (in-phase and out-of-phase) is less pronounced compared to **4**. A detailed analysis of the displacement vectors revealed that ν_1 can approximately be assigned to the movement of the N2═N3 double bond (see

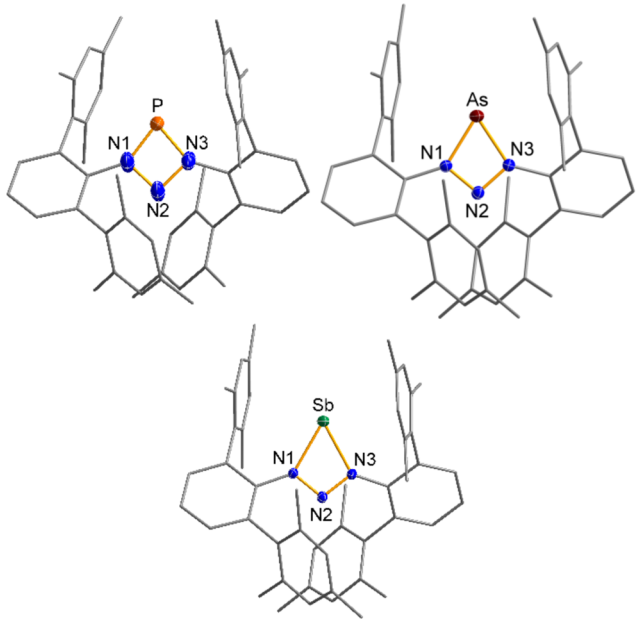

Figure 2. Molecular structures of **4P**, **4As**, and **4Sb** (see Table 2 for metrical parameters). Thermal ellipsoids are drawn at 50% probability (173 K).

Table 1. Vibrational Spectroscopic Data for 2 and 4[a]

	2As	2Sb	2Bi	4As	4Sb
$\nu_{1,NN}$	1425	1423	1421	1447	1440
$\nu_{2,NN}$	1259	1267	1261	1267	1269

[a]Approximate assignments based on DFT computations.

Figure 1), while ν_2 corresponds to the vibration of the N1–N2 single bond. Due to strong coupling in case of the higher symmetric species **4** (the double bond is delocalized along the NNN unit), ν_1 can be assigned to the asymmetric and ν_2 to the symmetric stretching mode.

4As and **4Sb** can be prepared in bulk and are thermally stable up to well above 100 °C in the solid state and decompose without melting (T_{dec}: **4P** 147 °C,[40] **4As** 148 °C, **4Sb** 157 °C). Crystals of **4E** rapidly decompose when traces of water or oxygen are present. In benzene solution at ambient conditions, none of the compounds **4P**, **4As**, and **4Sb** showed signs of decomposition according to NMR data. However, in boiling benzene already after 24 h considerable amounts of decomposition products were identified, among them, e.g., $TerNH_2$.

MOLECULAR STRUCTURES

The experimental structures of the four-membered formal *cyclo*-pnicta-triazanediyls (also known as triazapnictetes) and their starting materials, respectively, are shown in Figures 1 and 2.

The structures of the predominantly ionic triazenide **1** feature geometric parameters that are well within the range of known triazenides.[32−37] Due to a symmetric coordination mode, the N–N bonds are consimilar and vary only slightly upon changing the coordinated solvent molecule (cf. SI; ether solvate: 1.318(1), 1.311(1); thf solvate: 1.314(2), 1.314(2) Å). The N–N–N angle amounts to 107.5(1) (Et_2O solvate) and 107.9(1)° (thf solvate), respectively. Upon incorporation of the pnictogen chloride moieties, the molecular structures of **2As**, **2Sb**, and **2 Bi** feature clearly distinguishable N–N single (N1–

DOI: 10.1021/jacs.5b00959
J. Am. Chem. Soc. 2015, 137, 3975−3980

Table 2. Experimental (Computed)[b] Structural Data for 4E[a]

	4P	4As	4Sb	4Bi
N1−N2	1.352(1.329)	1.341(1.314)	1.315(1.301)	(1.293)
N1−E	1.685(1.755)	1.891(1.907)	2.078(2.147)	(2.282)
N3−E	1.687(1.755)	1.892(1.907)	2.105(2.147)	(2.282)
N2···E	2.248(2.344)	2.471(2.467)	2.635(2.678)	(2.794)
N1−N2−N2	96.7(95.7)	98.4(98.3)	103.4(104.7)	(107.5)
N1−E−N3	73.7(68.3)	64.8(63.8)	59.5(57.4)	(54.4)
β[c]	0.15	0.10	0.06	0.00
BO(N2···E)	0.40	0.30	0.00	0.00
NICS(o)	−2.1	−1.5	0.0	2.3
$\Sigma\pi$e	5.859	5.863	5.861	5.856

[a]Bond lengths in Å, angles in °. [b]Optimization for the model compound [E(μ-NPh)$_2$N] at M062X/aug-cc-pvdz, pseudopotentials for Sb: ECP28MDF and Bi: ECP60MDF. [c]$\beta = 2\ c_2^2/(c_1^2 + c_2^2)$.[48]

N2, 1.352(2), 1.335(3), 1.318(2) Å) and double bonds (N2−N3, 1.270(2), 1.282(2), 1.289(2) Å). The N_1−E distances are found in the typical range for such single bonds (**2As** 1.937(1), **2Sb** 2.153(1), **2Bi** 2.286(1) Å, cf. Σr_{cov}(E−N) 1.92, 2.11, 2.22 Å), while the N_3−E contacts are considerably longer (2.344(1), 2.408(2), 2.451(2) Å). Judged from the molecular geometry, the compounds **2** are closely related to known species incorporating guanidinate or amidinate substituents on pnictogen chloride moieties, which were investigated by the groups of Dehnicke,[41] Jones,[42] Schulz,[43] and Ragogna.[44]

In **2E** (E = As, Sb, Bi), a contact within the sum of van der Waals radii (E···centroid 3.234, 3.166, 2.971 Å) indicates additional stabilization due to weak interactions with the mesityl groups. In contrast, **2P** was not stable and rearranged to **3P** by intramolecular oxidation of P^{III} to P^{V}. Hence, the P−N distances are rather short: The structure features a N_1−P double bond (1.498(7) Å) and a considerably longer N_2−P single bond (1.743(8) Å). The N_2−N_3 bond (1.194(17) Å) corresponds to a typical double bond (Σr_{cov}(N═N) = 1.20 Å). The NPNN structural motif is located in a plane as expected for conjugated double bonds.

Species **4E** obtained after reduction exhibit planar kite-shaped four-membered N_3E heterocycles with almost two equal E−N bond lengths (E = P: 1.640(3), cf. Σr_{cov}(P−N) = 1.82 Å; As: 1.891(1), Σr_{cov}(As−N) = 1.92 Å and Sb: 2.078(1), Σr_{cov}(Sb−N) = 2.11 Å)[45] which is indicative of only a small amount of double bond character. The N1−N2 and N2−N3 bond lengths are consimilar again (**4As** 1.341(2), 1.337(2); **4Sb** 1.326(2), 1.326(2) Å). It is interesting to compare the transannular N2···E distances, increasing along P (2.25) < As (2.47) < Sb (2.64) < Bi (computed 2.79 Å), which is accompanied by decreasing N1−E−N3 angles and increasing N1−N2−N3 angles (Table 2). These short transannular N2···E distances are significantly shorter than the sum of the van der Waals radi (P: 3.35, As: 3.40, Sb: 3.61, Bi: 3.62 Å) but much longer than the sum of the covalent radii. It is noteworthy to mention that the metric parameters of the NNN and NNE moieties of **4Sb** and **4Bi** resemble those of the lithium salt **1** (e.g., **1**: N1−N2−N3 107.9(1)° vs **4Bi** 107.5°; Table S5), while deviations are more pronounced in **4P** and **4As** (Table 2), supporting the dominantly ionic bonding situation in **4Sb** and **4Bi** as discussed before.

A closer look at the secondary interactions revealed that the N_3E heterocycles are well protected inside the pocket formed by the two terphenyl substituents. However, as observed for the dichloro species **2E** (Figure 1), the dicoordinate pnictogen is stabilized by secondary interactions with two mesityl groups (e.g., E···centroids; As 3.508, 3.480, Sb 3.465, 3.437 Å; while in **2E** only one group interacts with the ECl_2 moiety (E···centroid, E = As 3.234; Sb 3.166 Å, Bi 2.971 Å). This type of π interactions (also referred to as Menshutkin-type complexes)[46] is more pronounced the heavier the pnictogen, as concluded from the pnictogen···centroid distances, which are well within the range of van der Waals radii. Moreover, in the case of **2E** species additional secondary interactions can be assumed between the negatively charged terminal N3 atom and the positive E center since rather short N3···E distances are found (N3···E: E = As 2.344(1), Sb 2.408(2), Bi 2.451(2) Å), which are considerably longer than the sum of the covalent radii but much shorter than the sum of the van der Waals radii.

■ COMPUTATIONAL STUDIES

It is known that biradicals such as [(μ-NTer)E]$_2$ (E = P, As) or [As(μ-NTer)$_2$P] can activate small molecules bearing double or triple bonds.[5,6,47] In contrast to these known biradicaloids neither molecules containing double bonds (alkenes, diazenes) nor alkynes (acetylene, phosphaalkynes) reacted with **4E** at ambient temperatures clearly indicating no significant reactivity as expected for a typical biradicaloid, in accord with the picture of a pnictogen(I) center coordinated by a chelating anionic triazenide ligand. To further support this view, computations at the M06-2X/aug-cc-pvdz and CASSCF(2,2) level of theory were carried out for the model systems [E(μ-NPh)$_2$N] with relativistic pseudopotentials applied for Sb and Bi (CASSCF = complete active space multiconfiguration self-consistent field, see SI for details).

CASSCF(2,2) computations for [E(μ-NPh)$_2$N] also indicate that the biradical character ($\beta = 2\ c_2^2/(c_1^2 + c_2^2)$)[48] is considerably smaller compared to [(μ-NTer)E]$_2$ (E = P, As) or [As(μ-NTer)$_2$P] (between 25−32%),[49] decreasing along the series **4P** (15%) > **4As** (10%) > **4Sb** (6%) > **4Bi** (0%). Hence, in agreement with natural resonance theory (NRT),[50,51] species such as **4E** are better understood as zwitterions according to the resonance depicted in Scheme 1 (see also Figure 3 and Table S19). Molecular orbital (MO), natural bond orbital (NBO), and electron localization function (ELF) data also manifest the decreasing delocalization of the lone pair localized at the pnictogen E along P > As > Sb > Bi (Table S22). The electronic situation on the reduced species **4E** is characterized by a π-type-HOMO (bonding along NEN but transannularly antibonding) and a π^*-type-LUMO (LUMO+1 for **4Sb** and **4Bi**: antibonding along NEN and NNN but transannularly bonding, Figure 4). However, the HOMO is more strongly localized at the pnictogen center the heavier E, while the π^*

DOI: 10.1021/jacs.5b00959
J. Am. Chem. Soc. 2015, 137, 3975−3980

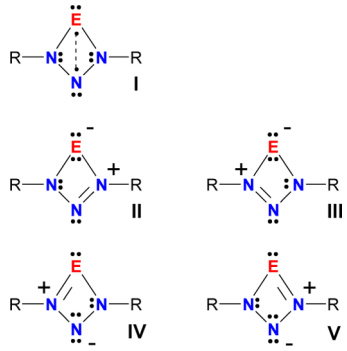

Figure 3. Most important Lewis representations according to NRT computations.

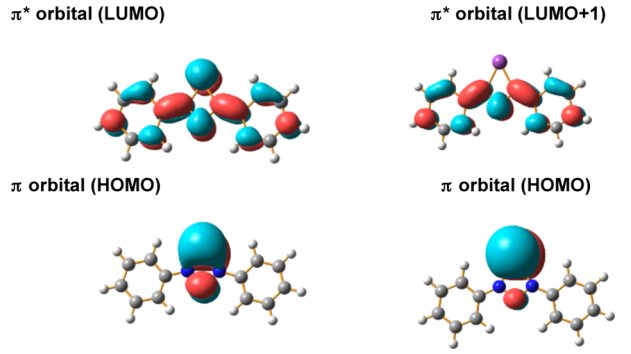

Figure 4. Electronic structure of **4P** (left) and **4Bi** (right).

MO with the transannular bonding situation becomes more strongly localized along the NNN moiety the heavier the pnictogen with very small coefficients for the Sb and Bi species. Hence, a strong biradical character (a larger contribution of the π^* MO to the overall wave function) is accompanied by a larger transannular bonding interaction as displayed by the E···N2 bond order decreasing along P (0.4) > As (0.3) > Sb (0.0) > Bi (0.0). The ELF function clearly indicates stronger localization of the two lone pairs (in-plane s-type and out-of-plane p-type lone pair) at the pnictogen in the order from P to Bi as displayed by the characteristic occurrence of two maxima in the ELF at 0.8 above and below the N_3E plane (Figure 5). The ELF function and NBO data show strongly polarized bonds between N and E. The bond polarization increases, the heavier the pnictogen is (P: 61, As: 65, Sb: 73 and Bi: 73% ionicity in the E−N bonds).

In the light of all these arguments above, the heavier species **4Sb** and **4Bi** might be better referred to as chelate complexes of a bulky triazenide anion with a E^+ cation bearing two localized lone pairs, while **4P** and **4As** feature some covalency in the σ and π electronic system. Although the number of π electrons amounts to almost six for all systems ($\Sigma\pi e$ = 5.9, Table 2), only for **4P** and **4As** significant delocalization is indicated by computations (Table S21, Figures 3 and 4) stabilizing the biradical character. Even though there are six π electrons present in all considered N_3E heterocycles, NICS(0) values indicate no significant aromaticity (Table 2, NICS = nucleus-independent chemical shift). This provides another difference to biradicaloid cyclobutane derivatives, for which aromaticity has been discussed.[5,6,52]

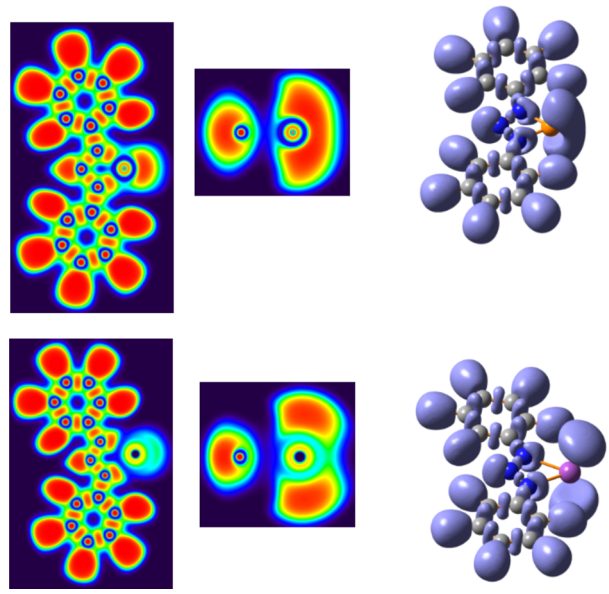

Figure 5. Left: 2D cross section through the ring plane of the ELF; middle section: perpendicular to the plane; and right: 3D representation of the ELF at 0.80 (top: **4P**, bottom **4Bi**).

CONCLUSION

In summary, a new type of four-membered N_3E heterocycles was prepared by reduction of triazenide-substituted pnictogen chlorides. Over the past 120 years[1] only a very small number of neutral binary four-membered ring molecules of the type $R_2N_xE_y$ (E = P − Bi; $x + y = 4$; x and y = 1−3) containing only the heavier pnictogens and nitrogen have been isolated and fully characterrized. Only two are known of the $R_2N_2E_2$ type: $[(\mu\text{-NR})E]_2$ (E = P, As; R = Ter, Hypersilyl)[5,6] but no representative of the nitrogen-rich R_2N_3E series ($[E(\mu\text{-NTer})_2N]$). All these classes of planar four-membered N_3E ring system have electronic structures that are related to those of aromatic hydrocarbons, which have six π electrons and therefore formally obey the Hückel rule. However, these $[E(\mu\text{-NTer})_2N]$ heterocycles feature a zwitterionic bond situation rather than a large biradical character contrary to the situation found in the cyclobutanediyl analogs: $[(\mu\text{-NR})E]_2$ (E = P, As). It is interesting to note that N_3P four-membered rings with a PR_3 moiety are discussed as Staudinger intermediates in the reaction of an azide with PPh_3.[53] Future studies may be concerned with the application of **4E** in trans-metalation reactions, complexation of transition metal compounds as well as the selective elimination of molecular nitrogen to in situ generate NE fragments, which can be further utilized in heterocyclic chemistry.

EXPERIMENTAL SECTION

General Information. All manipulations were carried out under oxygen- and moisture-free conditions under argon using standard Schlenk or drybox techniques. Benzene, diethyl ether, and tetrahydrofuran were dried over Na and freshly distilled prior to use. TerI, $TerN_3$, and KC_8 were prepared according to literature procedures.[39,54] PCl_3 and $AsCl_3$ were dried over P_4O_{10}, distilled, and degassed prior to use. $SbCl_3$ and $BiCl_3$ were purified by sublimation. Full Details can be found in the SI.

Synthesis of **1**. To a suspension of TerI (704 mg, 1.60 mmol) in 8 mL diethyl ether, *n*-BuLi (0.64 mL, 1.62 mmol, 2.5M) is added dropwise at 0 °C. The resulting colorless solution is stirred for 90 min at the same temperature. Afterward, the solution is treated with $TerN_3$

DOI: 10.1021/jacs.5b00959
J. Am. Chem. Soc. 2015, 137, 3975−3980

(560 mg, 1.58 mmol) and dissolved in 10 mL of diethyl ether. The reaction mixture immediately turns yellow and is allowed to warm to ambient temperature and stirred for 3 h. In the process, the color becomes more intense, and a yellow solid precipitates. The solution is filtered, and the precipitate is dried in vacuo for 1 h. The filtrate is stored at 4 °C overnight, resulting in the deposition of yellow crystals. The combined solids are dried in vacuo, yielding 960 mg (1.28 mmol, 81%) of the product. Recrystallization from diethyl ether or thf affords crystals suitable for X-ray structure elucidation. Mp: 168 °C (dec.). EA for $C_{52}H_{60}N_3LiO$ found (calcd): C 82.73 (83.27), H 7.90 (8.06), N 5.64 (5.61). ^{1}H NMR (298 K, C_6D_6, 250.1 MHz): 0.45 (t, $^3J_{HH}$ = 6.6 Hz, 6 H, CH_2-CH_3), 1.99 (s, 24 H, *o*-CH_3), 2.18 (s, 12 H, *p*-CH_3), 2.71 (q, $^3J_{HH}$ = 6.8 Hz, 4 H,), 6.81 (s, 8 H, CH_{Mes}), 6.86 (m, 6 H, CH_{ar}). $^{13}C\{^1H\}$ NMR (298 K, CD_2Cl_2, 62.9 MHz): 13.63 (s, CH_2-CH_3), 21.19 (s, *o*-CH_3), 21.80 (s, *p*-CH_3), 67.03 (s, CH_2-CH_3), 122.02 (s, CH), 128.16 (s, CH), 130.22 (s, CH), 132.86 (s), 134.59 (s), 135.85 (s), 140.40 (s), 147.06 (s).

Synthesis of ***2As***. A suspension of $Ter_2N_3Li{\cdot}Et_2O$ (1290 mg, 1.72 mmol) in 25 mL of diethyl ether is frozen in a bath of liquid nitrogen. To the frozen yellow suspension, $AsCl_3$ (450 mg, 2.48 mmol) is slowly added via syringe. The reaction flask is warmed to ambient temperature and stirred for 2 h. Volatiles are then removed in vacuo. Benzene (30 mL) is added, and the suspension is filtered (G4). The residue is washed by back-distillation of the solvent. The yellow filtrate is then concentrated to incipient crystallization and then left undisturbed overnight, which leads to the deposition of large yellow crystals. The mother liquor is removed via syringe, and the solid is dried in vacuo, yielding 1319 mg (1.48 mmol, 86%) of the product. Mp: 132 °C (dec.). EA for $C_{48}H_{50}N_3AsCl_2$ found (calcd): C 70.23 (70.76), H 6.71 (6.19), N 5.65 (5.16). ^{1}H NMR (298 K, CD_2Cl_2, 250.1 MHz): 1.96 (br s, 24 H, *o*-CH_3), 2.27 (s, 12 H, *p*-CH_3), 6.83 (s, 8 H, *m*-CH_{Mes}), 6.97 (m, 4 H, *m*-CH), 7.31 (t, $^3J_{HH}$ = 7.6 Hz, 2 H, *p*-CH). $^{13}C\{^1H\}$ NMR (298 K, CD_2Cl_2, 62.9 MHz): 20.53 (s, *o*-CH_3), 21.15 (s, *p*-CH_3), 121.76 (s, CH), 122.36 (s, CH), 123.47 (s, CH), 127.65 (s, CH), 128.35 (s, CH), 128.73 (s), 128.90 (s, CH), 129.03 (s, CH), 129.66 (s, CH), 130.13 (s, CH), 130.27 (s, CH), 134.37 (s), 136.00 (s), 136.78 (s), 137.08 (s), 137.27 (s), 138.23 (s), 139.79 (s). UV−vis (λ_{max}, nm): 341, 383.

Synthesis of ***2Sb***. To $Ter_2N_3Li{\cdot}Et_2O$ (811 mg, 1.081 mmol) in 10 mL benzene, $SbCl_3$ (248 mg, 1.087 mmol) in 5 mL benzene is added dropwise via syringe. The resulting suspension is stirred for further 90 min at ambient temperature and then filtered over a sinter padded with kieselguhr (G4). The residue is washed repeatedly with benzene (3x 3 mL). The filtrate is concentrated to incipient crystallization and left undisturbed for 2 days, which results in the deposition of yellow crystals suitable for X-ray structure elucidation. The mother liquor is removed via syringe and the solid dried in vacuo, yielding 681 mg of the product (0.756 mmol, 70%). Mp: 169 °C (dec.). EA for $C_{54}H_{56}N_3SbCl_2$ (C_6H_6 solvate) found (calcd): C 68.65 (69.02), H 5.71 (6.01), N 4.52 (4.47). EA for $C_{54}H_{55}N_3FSbCl_2$ (C_6H_5F solvate) found (calcd): C 67.56 (67.72), H 5.81 (5.79), N 3.36 (4.39). ^{1}H NMR (298 K, C_6D_6, 250.1 MHz): 1.96 (br s, 24 H, *o*-CH_3), 2.17 (s, 12 H, *p*-CH_3), 6.76 (d, $^3J_{HH}$ = 7.7 Hz, 4 H, *m*-CH), 6.83 (s, 8 H, *m*-CH_{Mes}), 6.92 (t, $^3J_{HH}$ = 7.6 Hz, 2 H, *p*-CH). $^{13}C\{^1H\}$ NMR (298 K, C_6D_6, 62.9 MHz): 21.45 (s, *p*-CH_3), 22.06 (s, *o*-CH_3), 128.25 (s, CH), 129.01 (s, CH), 129.26 (s, CH), 129.40 (s, CH), 130.48 (s, CH), 130.58 (s, CH), 130.99 (s, CH), 136.11 (s), 137.20 (s), 137.42 (s), 137.50 (s), 137.62 (s), 138.47 (s), 139.38 (s). UV−vis (λ_{max}, nm): 296, 352.

Synthesis of ***2Bi***. $Ter_2N_3Li{\cdot}Et_2O$ (565 mg, 0.753 mmol) and $BiCl_3$ (238 mg, 0.755 mmol) were combined as solids. To the mixture, 10 mL benzene is added and vigorously stirred at ambient temperature for 3 h, which leads to the formation of an orange suspension. Afterward, the suspension is filtered over a sinter padded with kieselguhr (G4). The residue is washed with benzene (3 × 2 mL), and the filtrate is concentrated to incipient crystallization (∼1 mL). After undisturbed overnight storage at ambient temperature, large orange crystals deposit. The mother liquor is removed via syringe, and the solid is dried in vacuo, yielding 402 mg (0.424 mmol, 56%) of the product. Mp: 179 °C (dec.). EA for $C_{48}H_{50}N_3BiCl_2$ found (calcd): C 60.21 (60.76), H 5.33 (5.31), N 4.43 (4.43). ^{1}H NMR (298 K, C_6D_6, 250.1 MHz): 1.99 (br s, 24 H, *o*-CH_3), 2.15 (s, 12 H, *p*-CH_3), 6.78 ($^3J_{HH}$ = 7.6 Hz, 4 H, *m*-CH), 6.81 ($^3J_{HH}$ = 7.6 Hz, 2 H, *p*-CH), 6.85 (s, 8 H, *m*-CH_{Mes}). $^{13}C\{^1H\}$ NMR (298 K, C_6D_6, 62.9 MHz): 21.40 (s, *p*-CH_3), 22.15 (s, *o*-CH_3), 128.19 (s, CH), 128.92 (s, CH), 129.40 (s, CH), 130.56 (s, CH), 137.24 (s), 137.63 (s), 137.79 (s), 138.09 (s), 141.22 (s).

Synthesis of ***3P***. A suspension of $Ter_2N_3Li{\cdot}Et_2O$ (600 mg, 0.8 mmol) in 15 mL of diethyl ether is frozen in a bath of liquid nitrogen. To the frozen yellow suspension, PCl_3 (510 mg, 3.7 mmol) is slowly added via syringe. The reaction flask is stored at −196 °C for further 15 min. Afterward, the nitrogen bath is removed, which leads to a dark-red solution when warmed to room temperature. The reaction mixture is stirred at ambient temperatures for 2 h. After completion of the reaction, volatiles are removed in vacuo. The dark-red residue is extracted with 10 mL of *n*-hexane by repeated back-distillation. The red filtrate is dried in vacuo, and the resulting precipitate is dissolved in 5 mL of benzene, which then is concentrated until crystallization commences and left undisturbed overnight, resulting in the deposition of red block-shaped crystals (145 mg, 0.19 mmol, 24%). Mp: 125 °C (dec.). EA for $C_{48}H_{50}N_3PCl_2$ found (calcd): C 73.98 (74.79), H 6.32 (6.54), N 5.37 (5.45). ^{1}H NMR (298 K, CD_2Cl_2, 250.1 MHz): 1.76 (s, 12 H, *o*-CH_3), 1.92 (s, 12 H, *o*-CH_3), 2.23 (s, 6 H, *p*-CH_3), 2.27 (s, 6 H, *p*-CH_3), 6.77 (s, 8 H, *m*-CH_{Mes}), 6.93 (m, 2 H, *m*-CH), 7.00 (br s, 1 H, *p*-CH), 7.16 (d, $^3J_{H-H}$ = 7.6 Hz, 2 H, *m*-CH), 7.54 (t, $^3J_{H-H}$ = 7.5 Hz, 1 H, *p*-CH). ^{31}P NMR (298 K, CD_2Cl_2, 121.5 MHz): −45.9 (s).

Synthesis of ***4As***. $Ter_2N_3AsCl_2$ (241 mg, 0.270 mmol) and Mg (60 mg, 2.46 mmol) are combined as solids. Then, 10 mL of THF are added, which results in a yellow solution, which is then stirred overnight (12 h) with a glass stirring bar. Within time, the solution becomes slightly darker yellow. The solvent is removed in vacuo and the residue is extracted with benzene (2 × 10 mL, G4). The filtrate is then concentrated (∼1 mL) and left undisturbed until yellow crystals have deposited. The mother liquor is decanted and removed by syringe, and the crystals are dried in vacuo, yielding 158 mg (0.213 mmol, 78%) of the product. Possible impurities can be removed by sublimation up to 135 °C. Mp: 148 °C (dec.). EA for $C_{51}H_{53}N_3As$ (benzene hemisolvate) found (calcd): C 78.04 (78.24), H 6.48 (6.82), N 5.32 (5.37). ^{1}H NMR (298 K, C_6D_6, 250.1 MHz): 1.96 (s, 24 H, *o*-CH_3), 2.21 (s, 12 H, *p*-CH_3), 6.78 (s, 8 H, CH_{Mes}), 6.79 (m, 4 H, *m*-CH), 6.86 (m, 2 H, *p*-CH). $^{13}C\{^1H\}$ NMR (298 K, C_6D_6, 62.9 MHz): 21.15 (s, *o*-CH_3), 21.64 (s, *p*-CH_3), 125.5 (s, CH), 128.93 (s, CH_{Mes}), 130.54 (s, CH), 132.23 (s), 134.36 (s), 135.91 (s), 137.16 (s), 137.34 (s), 138.99 (s), 139.82 (s), 142.31 (s), 145.75 (s). UV−vis (λ_{max}, nm): 332, 413.

Synthesis of ***4Sb***. 434 mg $Ter_2N_3SbCl_2$ (0.462 mmol) were dissolved in benzene (8 mL). 130 mg (0.962 mmol) KC_8 were added at ambient temperature. The suspension was stirred for further 3 h at ambient temperature and became red from initially yellow. Afterward, the suspension is filtered through a sinter padded with kieselguhr (G4). The residue was washed with 3 mL benzene. The combined filtrate was concentrated to incipient crystallization (1.5 mL) and left undisturbed overnight, which afforded red block-shaped crystals suitable for X-ray structure elucidation (223 mg, 0.282 mmol, 61%). Mp: 152 °C (dec.). EA for $C_{48}H_{50}N_3Sb$ found (calcd): C 72.92 (72.91), H 6.41 (6.37), N 5.13 (5.31). ^{1}H NMR (298 K, C_6D_6, 250.1 MHz): 2.05 (s, 24 H, *o*-CH_3), 2.16 (s, 12 H, *p*-CH_3), 6.73 (s, 8 H, *m*-CH_{Mes}), 6.75−6.81 (m, 6 H, *m*-/*p*-CH). $^{13}C\{^1H\}$ NMR (298 K, C_6D_6, 62.9 MHz): 21.63 (s, *p*-CH_3), 21.66 (s, *m*-CH_3), 124.96 (s, CH), 128.92 (s, CH), 129.11 (s, CH), 129.30 (s, CH), 130.51 (s), 130.74 (s), 135.66 (s), 137.31 (s), 137.45 (s), 141.36 (s). UV−vis (λ_{max}, nm): 352, 506.

■ ASSOCIATED CONTENT

Ⓢ Supporting Information

Additional experimental information, computational details, and crystallographic data. This material is available free of charge via the Internet at http://pubs.acs.org.

DOI: 10.1021/jacs.5b00959
J. Am. Chem. Soc. 2015, 137, 3975−3980

AUTHOR INFORMATION

Corresponding Author

*axel.schulz@uni-rostock.de

Notes

The authors declare no competing financial interest.

ACKNOWLEDGMENTS

The DFG (Deutsche Forschungsgemeinschaft, SCHU 1170/11-1) is gratefully acknowledged for financial support. A.H. thanks the GDCh (Gesellschaft Deutscher Chemiker) for financial support. The authors wish to thank M. Sc. Jonas Bresien for setting up and maintaining access to the cluster computer.

REFERENCES

(1) Michaelis, A.; Schroeter, G. *Chem. Ber.* **1894**, *27*, 490−497.
(2) He, G.; Shynkaruk, O.; Lui, M. W.; Rivard, E. *Chem. Rev.* **2014**, *114*, 7815−7880.
(3) Balakrishna, M. S.; Eisler, D. J.; Chivers, T. *Chem. Soc. Rev.* **2007**, *36*, 650−664.
(4) Stahl, L. *Coord. Chem. Rev.* **2000**, *210*, 203−250.
(5) Beweries, T.; Kuzora, R.; Rosenthal, U.; Schulz, A.; Villinger, A. *Angew. Chem., Int. Ed.* **2011**, *50*, 8974−8978.
(6) Demeshko, S.; Godemann, C.; Kuzora, R.; Schulz, A.; Villinger, A. *Angew. Chem., Int. Ed.* **2013**, *52*, 2105−2108.
(7) Breher, F. *Coord. Chem. Rev.* **2007**, *251*, 1007−1043.
(8) Abe, M. *Chem. Rev.* **2013**, *113*, 7011−7088.
(9) Ito, S.; Ueta, Y.; Ngo, T. T. T.; Kobayashi, M.; Hashizume, D.; Nishida, J.; Yamashita, Y.; Mikami, K. *J. Am. Chem. Soc.* **2013**, *135*, 17610−17616.
(10) Zhang, S.-H.; Xi, H.-W.; Lim, K. H.; Meng, Q.; Huang, M.-B.; So, C.-W. *Chem.—Eur. J.* **2012**, *18*, 4258−4263.
(11) Takeuchi, K.; Ichinohe, M.; Sekiguchi, A. *J. Am. Chem. Soc.* **2011**, *133*, 12478−12481.
(12) Kamada, K.; Ohta, K.; Shimizu, A.; Kubo, T.; Kishi, R.; Takahashi, H.; Botek, E.; Champagne, B.; Nakano, M. *J. Phys. Chem. Lett.* **2010**, *1*, 937−940.
(13) Wang, X.; Peng, Y.; Olmstead, M. M.; Fettinger, J. C.; Power, P. P. *J. Am. Chem. Soc.* **2009**, *131*, 14164−14165.
(14) Henke, P.; Pankewitz, T.; Klöpper, W.; Breher, F.; Schnöckel, H. *Angew. Chem., Int. Ed.* **2009**, *48*, 8141−8145.
(15) Ito, S.; Miura, J.; Morita, N.; Yoshifuji, M.; Arduengo, A. J. J. *Angew. Chem., Int. Ed.* **2008**, *47*, 6418−6421.
(16) Cox, H.; Hitchcock, P. B.; Lappert, M. F.; Pierssens, L. J.-M. *Angew. Chem.* **2004**, *116*, 4600−4604.
(17) Sebastian, M.; Hoskin, A.; Nieger, M.; Nyulaszi, L.; Niecke, E.; Nyulaszi, L. *Angew. Chem.* **2005**, *117*, 1429−1432.
(18) Amii, H.; Vranicar, L.; Gornitzka, H.; Bourissou, D.; Bertrand, G. *J. Am. Chem. Soc.* **2004**, *126*, 1344−1345.
(19) Cui, C.; Brynda, M.; Olmstead, M. M.; Power, P. P. *J. Am. Chem. Soc.* **2004**, *126*, 6510−6511.
(20) Scheschkewitz, D.; Amii, H.; Gornitzka, H.; Schoeller, W. W.; Bourissou, D.; Bertrand, G. *Science* **2002**, *295*, 1880−1881.
(21) Abe, M.; Adam, W.; Hara, M.; Hattori, M.; Majima, T.; Nojima, M.; Tachibana, K.; Tojo, S. *J. Am. Chem. Soc.* **2002**, *124*, 6540−6541.
(22) Grützmacher, H.; Breher, F. *Angew. Chem.* **2002**, *114*, 4178−4184.
(23) Schoeller, W. W.; Begemann, C.; Niecke, E.; Gudat, D. *J. Phys. Chem. A* **2001**, *105*, 10731−10738.
(24) Abe, M.; Adam, W.; Heidenfelder, T.; Nau, W. M.; Zhang, X. *J. Am. Chem. Soc.* **2000**, *122*, 2019−2026.
(25) Niecke, E.; Fuchs, A.; Baumeister, F.; Nieger, M.; Schoeller, W. W. *Angew. Chem.* **1995**, *107*, 640−642.
(26) Berson, J. A. *Science* **1994**, *266*, 1338−1339.
(27) Rajca, A. *Chem. Rev.* **1994**, *94*, 871−893.
(28) Borden, W. T. *Diradicals*; Wiley-Interscience: NewYork, 1982.
(29) Salem, L.; Rowland, C. *Angew. Chem.* **1972**, *84*, 86−106.
(30) Bauzá, A.; Escudero, D.; Frontera, A.; Streubel, R. *Organometallics* **2015**, *34*, 355−360.
(31) Seidl, M.; Kuntz, C.; Bodensteiner, M.; Timoshkin, A. Y.; Scheer, M. *Angew. Chem., Int. Ed.* **2015**, *54*, 2771−2775.
(32) Lee, H. S.; Niemeyer, M. *Inorg. Chem.* **2006**, *45*, 6126−6128.
(33) Lee, H.; Hauber, S.; Vinduš, D.; Niemeyer, M. *Inorg. Chem.* **2008**, *47*, 4401−4412.
(34) Lee, H.; Niemeyer, M. *Inorg. Chem.* **2010**, *49*, 730−735.
(35) Hauber, S.-O.; Lissner, F.; Deacon, G. B.; Niemeyer, M. *Angew. Chem.* **2005**, *117*, 6021−6025.
(36) Balireddi, S.; Niemeyer, M. *Acta Crystallogr., Sect. E: Struct. Rep. Online* **2007**, *63*, o3525−o3525.
(37) Wanner, M.; Scheiring, T.; Kaim, W.; Slep, L. D.; Baraldo, L. M.; Olabe, J. A.; Záliš, S.; Baerends, E. J. *Inorg. Chem.* **2001**, *40*, 5704−5707.
(38) Overländer, C.; Tirrée, J. J.; Nieger, M.; Niecke, E.; Moser, C.; Spirk, S.; Pietschnig, R. *Appl. Organomet. Chem.* **2007**, *21*, 46−48.
(39) Reiss, F.; Schulz, A.; Villinger, A.; Weding, N. *Dalton Trans.* **2010**, *39*, 9962−9972.
(40) The decomposition temperature was determined by DSC of mixed crystals of **4P** and **5**. It might be influenced by a reaction between the two species. The observed decomposition temperature is in the same range as for **4As** and **4Sb** and considerably lower than for **5**.
(41) Ergezinger, C.; Weller, F.; Dehnicke, K. *Z. Naturforsch.* **1988**, *43B*, 1119−1124.
(42) Green, S. P.; Jones, C.; Jin, G.; Stasch, A. *Inorg. Chem.* **2007**, *46*, 8−10.
(43) Lyhs, B.; Schulz, S.; Westphal, U.; Bläser, D.; Boese, R.; Bolte, M. *Eur. J. Inorg. Chem.* **2009**, *2009*, 2247−2253.
(44) Brazeau, A. L.; Nikouline, A. S.; Ragogna, P. J. *Chem. Commun.* **2011**, *47*, 4817−4819.
(45) Pyykkö, P.; Atsumi, M. *Chem.—Eur. J.* **2009**, *15*, 12770−12779.
(46) Schmidbaur, H.; Schier, A. *Organometallics* **2008**, *27*, 2361−2395.
(47) Hinz, A.; Kuzora, R.; Rosenthal, U.; Schulz, A.; Villinger, A. *Chem.—Eur. J.* **2014**, *20*, 14659−14673.
(48) Miliordos, E.; Ruedenberg, K.; Xantheas, S. S. *Angew. Chem.* **2013**, *125*, 5848−5851.
(49) Hinz, A.; Schulz, A.; Villinger, A. *Angew. Chem., Int. Ed.* **2014**, *54*, 668−672.
(50) Glendening, E. D.; Landis, C. R.; Weinhold, F. *J. Comput. Chem.* **2013**, *34*, 1429−1437.
(51) Glendening, E. D.; Weinhold, F. *J. Comput. Chem.* **1998**, *19*, 593−609.
(52) Bauzá, A.; Streubel, R.; Frontera, A. *Chem. Phys. Lett.* **2014**, *597*, 40−44.
(53) Tian, W. Q.; Wang, Y. A. *J. Org. Chem.* **2004**, *69*, 4299−4308.
(54) Savoia, D.; Trombini, C.; Umani-Ronchi, A. *Pure Appl. Chem.* **1985**, *57*, 1887−1896.

DOI: 10.1021/jacs.5b00959
J. Am. Chem. Soc. 2015, 137, 3975−3980